

Universal Scaling of Plasmon Coupling in Metal Nanostructures: Extension from Particle Pairs to Nanoshells

Prashant K. Jain[†] and Mostafa A. El-Sayed^{*†}

*Laser Dynamics Laboratory, School of Chemistry and Biochemistry,
Georgia Institute of Technology, Atlanta, Georgia 30332-0400*

Received June 23, 2007; Revised Manuscript Received July 23, 2007

ABSTRACT

It has been recently shown that the strength of plasmon coupling between a pair of plasmonic metal nanoparticles falls as a function of the interparticle gap scaled by the particle size with a near-exponential decay trend that is universally independent of nanoparticle size, shape, metal type, or medium dielectric constant. In this letter, we extend this universal scaling behavior to the dielectric core–metal shell nanostructure. By using extended Mie theory simulations of silica core–metal nanoshells, we show that when the shift of the nanoshell plasmon resonance wavelength scaled by the solid nanosphere resonance wavelength is plotted against the shell thickness scaled by the core radius, nanoshells with different dimensions (radii) exhibit the same near-exponential decay. Thus, the nanoshell system becomes physically analogous to the particle-pair system, i.e., the nanoshell plasmon resonance results from the coupling of the inner shell surface (cavity) and the outer shell surface (sphere) plasmons over a separation distance essentially given by the metal shell thickness, which is consistent with the plasmon hybridization model of Prodan, Halas, and Nordlander. By using the universal scaling behavior in the nanoshell system, we propose a simple expression for predicting the dipolar plasmon resonance of a silica–gold nanoshell of given dimensions.

Plasmonic nanostructures have attracted great interest in recent years due to their potential applications in molecular-specific imaging and spectroscopy,^{1–3} chemical and biological sensing,^{4–7} biomedicine,^{8–11} and nano-optical devices.¹² At the same time, a lot of fundamental interest has been focused on the interesting size, shape, composition, and medium dependence of the plasmon resonance in noble metal nanostructures.^{13–17} A classic example of this unique optical tunability is the dielectric core–metal shell nanostructure, especially the gold nanoshell studied in detail by the Halas and Nordlander groups,^{18–20} which consists of a silica core covered with a few nanometer thin gold layer. Other similar nanostructures include the gold sulfide core–gold shell,^{21–23} hollow metal shell,²⁴ and polystyrene core–metal shell nanostructures.^{25,26} The plasmon resonance of the metal shell nanostructure has been found to be strongly dependent on the relative dimensions of the metal shell and the dielectric core.¹⁸ By decreasing the thickness of the gold shell, the plasmon band of the nanoshell red-shifts from the visible region resonance (~ 520 nm) of the solid gold nanosphere toward the near-infrared region. Tunability of the plasmon resonance in the near-infrared region makes the nanoshell structure very useful for in vivo biomedical imaging and therapy applications^{8,9,27,28} because biological tissue shows

maximum optical transmissivity in the 650–900 nm region. Nanoshells also show promise for applications in nano-optical devices,²⁹ sensing,^{30,31} and surface-enhanced spectroscopy^{32,33} due to their strong and tunable plasmon resonance.

A nanostructure that shows optical tunability similar to metal nanoshell is the *hitherto* unrelated metal nanoparticle-pair system.^{34–40} The plasmon resonance of the gold nanoparticle pair can be red-shifted from the visible region resonance (ca. 520 nm) for an isolated gold nanosphere toward the near-infrared region by reducing the interparticle gap between the interacting particles for incident light polarized along the interparticle axis.^{37,39} The magnitude of this red-shift increases almost exponentially with decreasing interparticle gap.^{34,35,39} The plasmon shift scaled by the isolated-particle plasmon resonance plotted against the interparticle gap scaled by the particle dimension shows a near-exponential decay trend that is universally independent of nanoparticle size, shape, metal type, or surrounding dielectric medium.³⁹

In this letter, we present an interesting extension of this universal scaling behavior to the metal nanoshell structure. Extended Mie theory calculations show that as we move from a solid gold nanosphere to a nanoshell with decreasing shell thickness, there is an almost exponential red-shift in the plasmon resonance wavelength maximum. At the same time, the resonance wavelength shift is also dependent on the

* Corresponding author. E-mail: melsayed@gatech.edu. Telephone: 404-894-0292. Fax: 404-894-0294.

[†] Georgia Institute of Technology.

nanoshell size, i.e., the rise in the plasmon resonance red-shift with decreasing shell thickness is less steep for nanoshells with a larger size. However, when the shift of the nanoshell plasmon resonance wavelength scaled by the solid nanosphere resonance wavelength is plotted against the shell thickness scaled by the core radius, nanoshells with different dimensions show the same near-exponential decay trend. On the basis of this scaling behavior, we demonstrate the nanoshell system to be physically analogous to the particle-pair system. Our observation corroborates the “plasmon hybridization” model developed by Prodan et al.¹⁹ for explanation of the plasmon resonances in the nanoshell structure. In addition, our approach provides a simple expression to predict the dipolar plasmon resonance of a nanoshell with given core and shell dimensions.

In this work, the extinction efficiency (Q_{ext}) spectrum of a metal shell of thickness t surrounding a dielectric core of radius R was calculated in the visible–near-infrared region by using an extended Mie theory simulation scheme developed by Charamisinau et al.⁴¹ We used a refractive index of 1.45 for the core material corresponding to silica. For the gold shell, we used the wavelength-dependent complex refractive index of bulk gold.⁴² The surrounding medium was assumed to have a refractive index of 1.33 for liquid water. In the case where the shell thickness is reasonably smaller than the electronic mean free path of gold, the dielectric function needs to be corrected for increased electron scattering at the shell boundaries.²¹ The exact form of the correction is debated; however, it is known that the interface electron scattering results in increased damping of the resonance (i.e., lower extinction and increased linewidths); however, there is little effect on the plasmon resonance maximum position.⁴³ Because we are interested in the plasmon resonance positions, we have not included the correction. Nehl et al. have already demonstrated the ability of Mie theory, without inclusion of surface-scattering corrections, to simulate nanoshell plasmon resonances in good agreement with those determined from single-particle and solution-phase experiments.⁴⁴ We have ensured that the extended Mie theory calculation algorithm used in this work for core–shell particles shows excellent agreement with the results of Mie theory for homogeneous spheres for the three limiting cases: vanishing shell, vanishing core, and vanishing refractive index difference between core and shell materials.

Figure 1 shows the calculated extinction efficiency spectra for 80 nm diameter silica–gold nanoshells with varying gold shell thickness. The calculated spectrum for the 80 nm diameter solid nanosphere has a wavelength maximum λ_0 at 549 nm corresponding to its dipolar plasmon resonance. As the shell thickness t decreases from 40 nm (solid sphere) to 4 nm, the dipolar plasmon resonance progressively red-shifts. In addition, with decreasing shell thickness, the plasmon band extinction increases. At the smallest shell thickness, $t = 4$ nm, a small shoulder is observed around 690 nm, which corresponds to the quadrupolar/higher-order resonance mode.²⁰ These observed trends are very similar to those observed in a system of two interacting particles excited by light polarized along their interparticle axis.^{38,39} In the two-particle

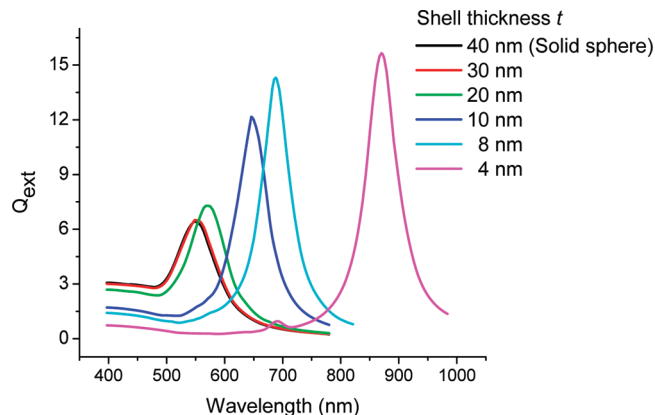


Figure 1. Extended Mie theory calculations of the extinction efficiency spectra of a 80 nm diameter silica core–gold nanoshell in water for different shell thickness: $t = 40$ nm (solid sphere), 30, 20, 10, 8, and 4 nm.

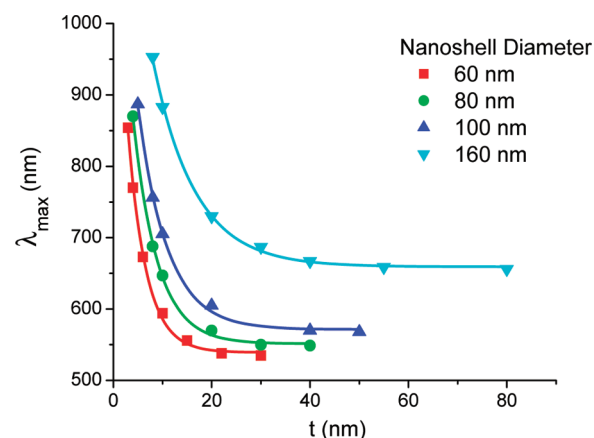


Figure 2. Calculated dipolar plasmon resonance wavelength maximum (λ_{max}) of a silica core–gold nanoshell in water as a function of shell thickness (t) for four different nanoshell diameters. The solid lines represent least-squares fits of the data to the single-exponential decay $y = y_0 + a \cdot \exp(-x/l)$, yielding $l = 3.71, 4.91, 5.93$, and 8.55 nm for nanoshell diameters = 60, 80, 100, and 160 nm, respectively.

system, as the interparticle gap decreases, there is a red-shift in the dipolar plasmon resonance along with an increase in the plasmon band extinction, and an emergence of the quadrupolar or higher-order modes at very small gap.³⁹

In fact, similar to the nanoparticle-pair system, there is a near-exponential red-shift in the dipolar plasmon resonance wavelength maximum with decreasing shell thickness (Figure 2). Figure 2 gives a comparison of this trend for four different nanoshell sizes, where it is evident that the rise in the plasmon red-shift with decreasing shell thickness is less steep for nanoshells with a larger size.

It must be noted that Oldenburg et al. have already elucidated by experiment and simulation the dependence of the silica core–gold nanoshell plasmon resonance on the shell thickness.¹⁸ They have also acknowledged the role of the total nanoshell size in determining the plasmon resonance. However, for the first time, we demonstrate a unique size scaling that exists in the nanoshell system analogous to that demonstrated in the particle-pair system. In Figure 3, we have plotted the fractional shift ($\Delta\lambda/\lambda_0$) of the nanoshell plasmon

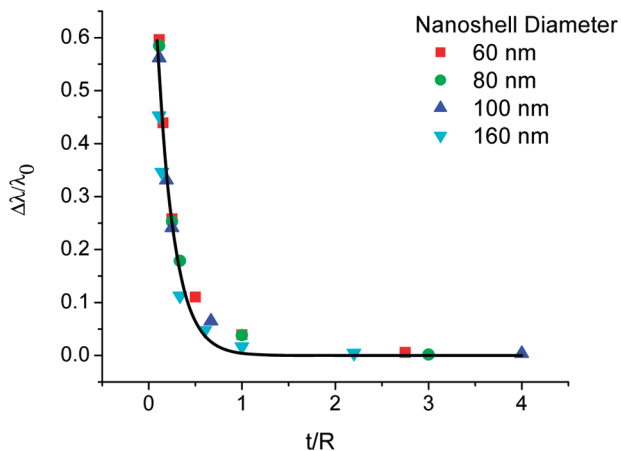


Figure 3. The fractional shift ($\Delta\lambda/\lambda_0$) of the dipolar plasmon resonance wavelength maximum of the silica core–gold nanoshell in water with respect to the solid gold nanosphere plasmon resonance maximum plotted against the ratio of the shell thickness to the core radius (t/R) for four different nanoshell diameters. The data points for the different nanoshell diameters fall on the same curve, given by the solid line, which is a least-squares fit ($R^2 = 0.962$) of the data to the single-exponential decay $y = a \cdot \exp(-x/\tau)$ with $\tau = 0.18 \pm 0.02$ and $a = 0.97 \pm 0.08$.

resonance wavelength with respect to the solid nanosphere resonance wavelength versus the shell thickness scaled by the core radius (t/R).⁴⁵ By applying this scaling, the trend becomes independent of the nanoshell dimensions. The exponential decay constant of this universal trend is 0.18 ± 0.02 . The decay constant does not seem to be affected much by a change in the material of the core or shell or the surrounding medium. For instance, the decay constants for 60 nm diameter hollow core–gold nanoshell in water, 60 nm diameter silica core–silver nanoshell in water, and 60 nm diameter silica–gold nanoshell in air are close (Supporting Information, Figures S1–S3). The amplitude of the fractional shift, however, does depend on the dielectric properties of the core, shell, and environment. In general, we find that higher dielectric constant of the core or that of the surrounding medium leads to a larger fractional shift,⁴⁶ which is similar to the observation in the particle-pair system.³⁹ As also proposed for the particle-pair system,^{7,34,39} using silver as the material of the plasmonic shell also leads to a larger resonance shift as compared to that of gold (Supporting Information, Figure S3) due to the stronger electromagnetic fields in silver. The line widths for silver are also much narrower.

This interesting parallel between the particle-pair system and the nanoshell structure is very well reconciled with the plasmon hybridization model, which was developed by Prodan et al.¹⁹ for explanation of the physical origin of the tunable plasmon resonance in metal nanoshells. As per this model, the metal nanoshell is a two-interface system, which supports two distinct plasmon modes: an outer shell-surface sphere mode and an inner shell-surface cavity mode, which couple/hybridize with each other, leading to a splitting into two new modes. The antisymmetric combination of these modes results in a higher-energy (blue-shifted) plasmon mode, while the symmetric combination results in a lower-

energy (red-shifted) plasmon mode, which lies in the visible–near-infrared region. The position of the visible–near-infrared resonance is thus determined by the extent of the splitting, in other words, the strength of the plasmon interaction. The metal shell thickness represents the distance over which this interaction takes place. The plasmon coupling strength between the cavity and sphere modes vanishes over the shell thickness t similar to the decay of the plasmonic field in the interparticle gap of the particle-pair system.

The plasmon coupling strength in the nanoparticle-pair system is determined by the strength of the near-field, which for dipolar interaction falls as the inverse cube of distance.^{38,39} At the same time, a higher value of the particle polarizability (which for the dipolar mode is proportional to the cube of the particle size) ensures stronger coupling. As a consequence, the fractional shift $\Delta\lambda/\lambda_0$ for the dipolar resonance of the nanoparticle-pair system has a functional dependence on $(s/D + 1)^{-3}$ (where s is the interparticle separation and D is the particle diameter) that can be approximated to an exponential decay.³⁹ Likewise, in the nanoshell system, we can expect the fractional shift of the dipolar resonance to be a function of $(t/R + 1)^{-3}$, where t is the shell thickness and R is the core radius. In other words, a larger core has a larger polarizability and a thinner shell ensures stronger near-field coupling, thus leading to a larger fractional plasmon shift. In fact, the dipolar resonance condition for a core–shell structure in the quasistatic limit is specified by:^{17,23}

$$\epsilon_c = -2\epsilon_s \frac{\epsilon_s(1-f) + \epsilon_m(2+f)}{\epsilon_s(1+2f) + 2\epsilon_m(1-f)} \quad (1)$$

where ϵ_c , ϵ_s , and ϵ_m are the dielectric constants of the core, shell, and medium, respectively, and f is the fraction of the volume of the core in the composite structure. It is interesting to note that f is essentially $(t/R + 1)^{-3}$. This analogy serves to qualitatively explain the similarity of the distance dependence and scaling behavior of plasmon coupling in the nanoshell structure to that in the particle-pair structure. Further analysis (Supporting information, Figure S4) shows that the fractional dipolar resonance shift for a silica core–gold nanoshell calculated from eq 1 when plotted against t/R shows a near-exponential decay with a decay constant of 0.19 ± 0.01 . The plasmon hybridization model by Prodan et al. also results in an expression where the nanoshell resonance frequency is a function of the core radius to shell radius ratio raised to the power $(2l + 1)$ where $l = 1, 2, \dots$, corresponding to the dipole, quadrupole, ..., etc.²² The plasmon hybridization model has also been shown to be valid for describing plasmonic coupling in nanoparticle dimers.⁴⁰

In addition to the plasmon resonance maximum position, we can also expect the extinction efficiency,¹⁶ ratio of scattering to absorption,¹⁶ resonance line width,⁴³ and refractive index sensitivity³¹ of the nanoshell system to have some defined functional dependence on f , at least within the limit of the quasistatic and dipole approximations. In the case of larger sizes, the complicating effect of electromagnetic retardation⁴³ and higher-order interactions²⁰ may result in some deviations from the universal dependence.

While we have approximated the plasmon coupling in the core-shell structure as well as the particle-pair by a dipole-dipole type interaction, which falls with distance d as $1/d^3$; in a more complete treatment, one should consider that the dipolar resonance mode of each pair-partner interacts with the higher-energy multipolar plasmon modes of the other partner, thus resulting in the formation of a hybridized “dipolar” plasmon mode with a mixed multipolar composition. In general, the interaction between a plasmon mode of order l and that of order l' falls with distance as $1/d^{l+l'+1}$. Thus, the complete multipolar interaction can be represented as a geometric series in $1/d$, which effectively reflects an exponential decay. While the approximation of dipole-dipole interaction works very well at relatively larger interaction distances, at smaller distances, the multipolar contribution to the interaction becomes increasingly important, thus leading to a “nondipolar” shift in the dipolar plasmon resonance.³⁹ While this is true for the particle-pair system, the spherical symmetry in the nanoshell system⁴⁷ allows only modes of the same angular momentum to interact (i.e., $l' = l = 0$). This is probably why a purely dipolar interaction (for example, eq 1) can be used to explain the dipolar nanoshell resonance with good quantitative agreement, unlike the particle-pair system.³⁹

In addition to providing fundamental insight into the nature of the plasmon coupling in the nanoshell structure, our extension of the scaling behavior of the plasmon coupling to the nanoshell system allows us to present a simple empirical expression to estimate the plasmon resonance extinction wavelength maximum λ_{\max} for a nanoshell of given dimensions. From the fit to the universal trend exhibited by silica-gold nanoshells in water (Figure 3), we get:

$$\frac{\Delta\lambda}{\lambda_0} = 0.97 \exp\left(\frac{-t/R}{0.18}\right) \quad (2)$$

where t is the gold shell thickness, R is the core radius, λ_0 is the plasmon extinction wavelength maximum of a solid sphere of the same size as the nanoshell, and $\Delta\lambda = \lambda_{\max} - \lambda_0$ is the shift of the nanoshell extinction wavelength maximum from the resonance maximum of this solid sphere. Hirsch et al. employed a nanoshell with a silica core of 110 nm diameter and a 10 nm gold shell thickness for in vivo cancer therapy.⁹ For this case, $\lambda_0 = 606$ nm from Mie theory for a 65 nm radius gold nanosphere. Thus, from eq 2 we get $\lambda_{\max} = 820$ nm, which agrees with the experimental extinction maximum of 820 nm. Equation 2 thus provides a simple design guideline (in lieu of detailed electrodynamic calculations) for tuning the nanoshell optical resonance in aqueous media, which would be useful for biomedical imaging and therapy applications in vivo. Note that the scaling behavior represented by eq 2 incorporates the dependence of the nanoshell plasmon resonance wavelength maximum on both the shell-to-core ratio and the total nanoshell volume, unlike earlier models.^{18,19} In addition, our analysis is based on a fully retarded Mie theory, which includes size-dependent electromagnetic retardation effects.

Thus, we have extended the universal scaling behavior of plasmon coupling from the particle-pair system to the metal

shell nanostructure, thus drawing a clear analogy between these two systems in corroboration of the plasmon hybridization model.

Acknowledgment. We thank the financial support of the NCI Center of Cancer Nanotechnology Excellence (CCNE) Award (U54CA119338). We thank Ivan Charamisinau for his program for Mie theory calculations of composite particles and Philip Laven for his program MiePlot based on the BHMIE algorithm.

Supporting Information Available: Plot of fractional plasmon shift versus ratio of shell thickness to core radius, calculated using extended Mie theory for (1) 60 nm diameter hollow core-gold nanoshell in water (Figure S1), (2) 60 nm diameter silica core-silver nanoshell in water (Figure S2), (3) 60 nm diameter silica core-gold nanoshell in air (Figure S3), and (4) from the quasistatic dipolar resonance condition for the nanoshell (Figure S4). This material is available free of charge via the Internet at <http://pubs.acs.org>.

References

- (1) El-Sayed, I. H.; Huang, X.; El-Sayed, M. A. *Nano Lett.* **2005**, *5*, 829–834.
- (2) Sokolov, K.; Follen, M.; Aaron, J.; Pavlova, I.; Malpica, A.; Lotan, R.; Richards-Kortum, R. *Cancer Res.* **2003**, *63*, 1999–2004.
- (3) Loo, C.; Hirsch, L. R.; Lee, M. H.; Chang, E.; West, J.; Halas, N.; Drezeck, R. *Opt. Lett.* **2005**, *30*, 1012–1014.
- (4) Alivisatos, A. P. *Nat. Biotechnol.* **2004**, *22*, 47–52.
- (5) Rosi, N. L.; Mirkin, C. A. *Chem. Rev.* **2005**, *105*, 1547–1562.
- (6) Haes, A. J.; Zou, S.; Schatz, G. C.; Van Duyne, R. P. *J. Phys. Chem. B* **2004**, *108*, 6961–6968.
- (7) Sonnichsen, C.; Reinhard, B. M.; Liphardt, J.; Alivisatos, A. P. *Nat. Biotechnol.* **2005**, *23*, 741–745.
- (8) Loo, C. A.; Lowery, A.; Halas, N.; West, J.; Drezeck, R. *Nano Lett.* **2005**, *5*, 709–711.
- (9) Hirsch, L. R.; Stafford, R. J.; Bankson, J. A.; Sershen, S. R.; Rivera, B.; Price, R. E.; Hazle, J. D.; Halas, N. J.; West, J. L. *Proc. Natl. Acad. Sci. U.S.A.* **2003**, *100*, 13549–13554.
- (10) Huang, X.; El-Sayed, I. H.; Qian, W.; El-Sayed, M. A. *J. Am. Chem. Soc.* **2006**, *128*, 2115–2120.
- (11) Jain, P. K.; El-Sayed, I. H.; El-Sayed, M. A. *Nano Today* **2007**, *2*, 18–29.
- (12) Maier, S. A.; Brongersma, M. L.; Kik, P. G.; Meltzer, S.; Requicha, A. A. G.; Atwater, H. A. *Adv. Mater.* **2001**, *13*, 1501–1505.
- (13) Kelly, K. L.; Coronado, E.; Zhao, L. L.; Schatz, G. C. *J. Phys. Chem. B* **2003**, *107*, 668–677.
- (14) El-Sayed, M. A. *Acc. Chem. Res.* **2001**, *34*, 257–264.
- (15) Link, S.; El-Sayed, M. A. *Int. Rev. Phys. Chem.* **2000**, *19*, 409–453.
- (16) Jain, P. K.; Lee, K. S.; El-Sayed, I. H.; El-Sayed, M. A. *J. Phys. Chem. B* **2006**, *110*, 7238–7248.
- (17) Bohren, C. F.; Huffman, D. R. *Absorption and Scattering of Light by Small Particles*; Wiley: New York, 1983.
- (18) Oldenburg, S. J.; Averitt, R. D.; Westcott, S. L.; Halas, N. J. *Chem. Phys. Lett.* **1998**, *28*, 243–247.
- (19) Prodan, E.; Radloff, C.; Halas, N. J.; Nordlander, P. *Science* **2003**, *302*, 419–422.
- (20) Oldenburg, S. J.; Jackson, J. B.; Westcott, S. L.; Halas, N. J. *Appl. Phys. Lett.* **1999**, *75*, 2897–2899.
- (21) Averitt, R. D.; Sarkar, D.; Halas, N. J. *Phys. Rev. Lett.* **1997**, *78*, 4217–4220.
- (22) Prodan, E.; Nordlander, P.; Halas, N. J. *Nano Lett.* **2003**, *3*, 1411–1415.
- (23) Zhou, H. S.; Honma, I.; Komiyama, H.; Haus, J. W. *Phys. Rev. B* **1994**, *50*, 12052–12056.
- (24) Sun, Y.; Mayers, B.; Xia, Y. *Adv. Mater.* **2003**, *15*, 641–646.
- (25) Shi, W.; Sahoo, Y.; Swihart, M. T.; Prasad, P. N. *Langmuir* **2005**, *21*, 1610–1617.
- (26) Liang, Z.; Susha, A.; Caruso, F. *Chem. Mater.* **2003**, *15*, 3176–3183.

- (27) Loo, C.; Lin, A.; Hirsch, L.; Lee, M.-H.; Barton, J.; Halas, N.; West, J.; Drezeck, R. *Technol. Cancer Res. Treat.* **2004**, *3*, 33–40.
- (28) O'Neal, D. P.; Hirsch, L. R.; Halas, N. J.; Payne, J. D.; West, J. L. *Cancer Lett.* **2004**, *209*, 171–176.
- (29) Sershen, S. R.; Mensing, G. A.; Ng, M.; Halas, N. J.; Beebe, D. J.; West, J. L. *Adv. Mater.* **2005**, *17*, 1366–1368.
- (30) Sun, Y.; Xia, Y. *Anal. Chem.* **2002**, *74*, 5297–5305.
- (31) Tam, F.; Moran, C.; Halas, N. J. *Phys. Chem. B* **2004**, *108*, 17290–17294.
- (32) Jackson, J. B.; Halas, N. J. *Proc. Natl. Acad. Sci. U.S.A.* **2004**, *101*, 17930–17935.
- (33) Tam, F.; Goodrich, G. P.; Johnson, B. R.; Halas, N. J. *Nano Lett.* **2007**, *7*, 496–501.
- (34) Gunnarsson, L.; Rindzevicius, T.; Prikulis, J.; Kasemo, B.; Käll, M.; Zou, S.; Schatz, G. C. *J. Phys. Chem. B* **2005**, *109*, 1079–1087.
- (35) Su, K. H.; Wei, Q.-H.; Zhang, X.; Mock, J. J.; Smith, D. R.; Schultz, S. *Nano Lett.* **2003**, *3*, 1087–1090.
- (36) Rechberger, W.; Hohenau, A.; Leitner, A.; Krenn, J. R.; Lamprecht, B.; Aussenegg, F. R. *Opt. Commun.* **2003**, *220*, 137–141.
- (37) Reinhard, B. M.; Siu, M.; Agarwal, H.; Alivisatos, A. P.; Liphardt, J. *Nano Lett.* **2005**, *5*, 2246–2252.
- (38) Jain, P. K.; Eustis, S.; El-Sayed, M. A. *J. Phys. Chem. B* **2006**, *110*, 18243–18253.
- (39) Jain, P. K.; Huang, W.; El-Sayed, M. A. *Nano Lett.* **2007**, *7*, 2080–2088.
- (40) Nordlander, P.; Oubre, C.; Prodan, E.; Li, K.; Stockman, M. I. *Nano Lett.* **2004**, *4*, 899–903.
- (41) Charamisinau, I.; Happawana, G.; Evans, G.; Rosen, A.; Hsi, R. A.; Bour, D. *Appl. Opt.* **2005**, *44*, 5055–5068.
- (42) Johnson, P. B.; Christy, R. W. *Phys. Rev. B* **1972**, *6*, 4370–4379.
- (43) Grady, N. K.; Halas, N. J.; Nordlander, P. *Chem. Phys. Lett.* **2004**, *399*, 167–171.
- (44) Nehl, C. L.; Grady, N. K.; Goodrich, G. P.; Tam, F.; Halas, N. J.; Hafner, J. H. *Nano Lett.* **2004**, *4*, 2355–2359.
- (45) Note that, in the present analysis, we have consistently used a lower bound on the t/R value of about 0.1 for the different nanoshell diameters.
- (46) Prodan, E.; Nordlander, P.; Halas, N. J. *Chem. Phys. Lett.* **2003**, *368*, 94–101.
- (47) Wang, H.; Wu, Y.; Lassiter, B.; Nehl, C. L.; Hafner, J. H.; Nordlander, P.; Halas, N. J. *Proc. Natl. Acad. Sci. U.S.A.* **2006**, *103*, 10856–10860.

NL071496M